

Model independent constraints on contact interactions from LEP2¹

A.A. Pankov^{a,b,c} and N. Paver^{c,2}

^a Pavel Sukhoi Technical University, Gomel 246746, Belarus

^b International Centre for Theoretical Physics, 34100 Trieste, Italy

^c Dipartimento di Fisica Teorica, Università di Trieste and
Istituto Nazionale di Fisica Nucleare, Sezione di Trieste, 34100 Trieste, Italy

Abstract

We quantitatively discuss the possibility of deriving model-independent constraints on the general four-fermion contact interaction couplings, from the currently available data on the two-fermion production processes $e^+e^- \rightarrow \mu^+\mu^-$, $b\bar{b}$ and $c\bar{c}$ with unpolarized initial beams. The method is essentially based on particular, simple, combinations of the measured total cross section and forward-backward asymmetry that allow partial separation of the helicity cross sections, and the combination of experimental data obtained at the different energies of TRISTAN, LEP1 and LEP2.

¹Partially supported by MURST (Italian Ministry of University, Scientific Research and Technology).

²E-mail address: nello.paver@ts.infn.it

High precision data on fermion-pair production by e^+e^- collisions at LEP is regarded both as a powerful test of the Standard Model (SM) and as an interesting tool to severely constrain the parameters of non-standard dynamics that might manifest themselves through deviations of the measured observables from the SM predictions [1].

In particular, this is the case of the $SU(3) \times SU(2) \times U(1)$ symmetric $eeff$ contact-interaction Lagrangian with helicity-conserving and flavor-diagonal fermion currents that can be expressed as [2]:

$$\mathcal{L} = \sum_{\alpha\beta} g_{\text{eff}}^2 \epsilon_{\alpha\beta} (\bar{e}_\alpha \gamma_\mu e_\alpha) (\bar{f}_\beta \gamma^\mu f_\beta), \quad (1)$$

where generation and color indices are not explicitly indicated, $\alpha, \beta = \text{L, R}$ denote left- or right-handed fermion helicities, and the parameters $\epsilon_{\alpha\beta} = \pm 1/\Lambda_{\alpha\beta}^2$ specify the chiral structure of the individual interactions, with $\Lambda_{\alpha\beta}$ some high energy scales that determine the size of the effects. Conventionally, the scales of Λ 's are chosen by conventionally fixing $g_{\text{eff}}^2/4\pi = 1$ as a reminder that this new interaction, originally proposed for compositeness, would become strong at the reaction energy $\sqrt{s} \sim \Lambda_{\alpha\beta}$. In fact, more generally, Eq. (1) can be considered as an effective Lagrangian that parametrizes the effects at the ‘low’ energy \sqrt{s} of any non-standard dynamics acting at the much larger scales $\Lambda_{\alpha\beta} \gg \sqrt{s}$, at the leading order in $\sqrt{s}/\Lambda_{\alpha\beta}$. In addition to the remnant compositeness binding force mentioned above, familiar examples are the exchanges of a heavy Z' [3] and of a heavy leptoquark [4]. From this point of view, the scales $\Lambda_{\alpha\beta}$ define the standard to compare the sensitivity of measurements to the various kinds of new interactions.

Referring to the processes under consideration ($f \neq e, t$):

$$e^+ + e^- \rightarrow f + \bar{f}, \quad (2)$$

once combined with the SM γ - and Z -exchanges, the contact Lagrangian \mathcal{L} should “indirectly” manifest itself by modifications of observables from the SM predictions and, clearly, the numerical comparison of such deviations to the experimental accuracies quantitatively determines the attainable reach in the free mass scales $\Lambda_{\alpha\beta}$ or, equivalently, the experimental sensitivity to the new coupling constants $\epsilon_{\alpha\beta}$.

In practice, the situation is complicated by the fact that, for a given flavor f , Eq. (1) defines eight individual, independent, models corresponding to the combinations of the four chiralities α, β with the \pm signs of the ϵ 's, and the general contact interaction could be any linear combination of these models. Accordingly, the aforementioned deviations of from the SM predictions simultaneously depend on all four-fermion effective couplings and, for a fixed value of the energy \sqrt{s} , their straightforward comparison to the experimental uncertainties *a priori* could only produce numerical correlations among the possible values of the different couplings, rather than separate, and restricted, allowed regions around the SM limit $\epsilon_{\alpha\beta} = 0$. This could be obtained only by a procedure based on suitable observables and/or the analysis of appropriate samples of experimental data.

Indeed, the simplest, and commonly adopted, procedure consists in assuming non-zero values for just one of the $\epsilon_{\alpha\beta}$ at a time, and in constraining it to a finite interval by

essentially a χ^2 fit analysis of the total cross section and the forward-backward asymmetry, while all the remaining parameters are set equal to zero [3, 5]. In this way, only tests of the aforementioned particular models can be performed.

On the other hand, as emphasized above, it is desirable to perform a general, and model-independent, kind of analysis of the experimental data that simultaneously includes all terms of Eq. (1) as free parameters and, at the same time, allows to disentangle their contributions to the basic observables to the largest possible extent in order to derive separate constraints. In particular, this procedure would avoid potential cancellations between different contributions that might considerably weaken the numerical constraints. The ideal solution to this problem would be represented by the longitudinal initial electron beam polarization, that would enable us to experimentally extract the individual helicity amplitudes $A_{\alpha\beta}$ of process (2), that by definition are directly related to the single $eeff$ contact coupling $\epsilon_{\alpha\beta}$ and, therefore, depend on the minimal set of free independent parameters [6]. Unfortunately, such a procedure cannot be applied to the LEP data, that refer to measurements of the total cross section σ and of the forward-backward asymmetry A_{FB} with unpolarized electron and positron beams.

In this case, we adopt an approach based on two particular observables, σ_+ and σ_- , that are simple combinations of the “conventional” ones σ and A_{FB} , and allow to partially disentangle the contributions of the terms with different chiralities in Eq. (1). Since the separation is only partial, by themselves σ_+ and σ_- would still lead to correlations among pairs of contact interaction couplings squared rather than a well-defined, and restricted, allowed region. This restricted area could be derived by a global analysis that supplements the recent LEP2 data on σ and A_{FB} with the measurements of the same observables at the quite different energies of LEP1 and of TRISTAN, taking advantage of the expected energy-dependence of the deviations from the SM due to the new interaction (1), entirely determined by well-known SM parameters.

Limiting ourselves to the cases $f \neq e, t$ and neglecting all fermion masses with respect to \sqrt{s} , the amplitude for process (2) is determined by the Born γ and Z exchanges in the s channel plus the contact-interaction term of Eq. (1). With θ the angle between the incoming electron and the outgoing fermion in the c.m. frame, the differential cross section reads [7]:

$$\frac{d\sigma}{d\cos\theta} = \frac{3}{8} [(1 + \cos\theta)^2 \sigma_+ + (1 - \cos\theta)^2 \sigma_-]. \quad (3)$$

In terms of helicity cross sections $\sigma_{\alpha\beta}$ (with $\alpha, \beta = \text{L, R}$):

$$\sigma_+ = \frac{1}{4} (\sigma_{\text{LL}} + \sigma_{\text{RR}}), \quad (4)$$

$$\sigma_- = \frac{1}{4} (\sigma_{\text{LR}} + \sigma_{\text{RL}}). \quad (5)$$

In Eqs. (4) and (5):

$$\sigma_{\alpha\beta} = N_C \sigma_{\text{pt}} |A_{\alpha\beta}|^2, \quad (6)$$

where $N_C \simeq 3(1 + \alpha_s/\pi)$ for quarks and $N_C = 1$ for leptons, respectively, and $\sigma_{\text{pt}} \equiv \sigma(e^+e^- \rightarrow \gamma^* \rightarrow l^+l^-) = 4\pi\alpha_{e.m.}^2/3s$. The helicity amplitudes $A_{\alpha\beta}$ can be written as

$$A_{\alpha\beta} = Q_e Q_f + g_\alpha^e g_\beta^f \chi_Z + \frac{s}{\alpha_{e.m.}} \epsilon_{\alpha\beta}, \quad (7)$$

where: $\chi_Z = s/(s - M_Z^2 + iM_Z\Gamma_Z)$ is Z propagator; $g_L^f = (I_{3L}^f - Q_f s_W^2)/s_W c_W$ and $g_R^f = -Q_f s_W^2/s_W c_W$ are the SM left- and right-handed fermion couplings of the Z with $s_W^2 = 1 - c_W^2 \equiv \sin^2 \theta_W$; Q_f are the fermion electric charges.

The “conventional” observables σ and A_{FB} are given by the relations:

$$\sigma = \sigma_+ + \sigma_- = \sigma_F + \sigma_B = \frac{1}{4}(\sigma_{\text{LL}} + \sigma_{\text{RR}} + \sigma_{\text{LR}} + \sigma_{\text{RL}}); \quad (8)$$

and

$$\sigma_{\text{FB}} \equiv \sigma A_{\text{FB}} = \sigma_F - \sigma_B = \frac{3}{4}(\sigma_+ - \sigma_-) = \frac{3}{16}(\sigma_{\text{LL}} + \sigma_{\text{RR}} - \sigma_{\text{LR}} - \sigma_{\text{RL}}). \quad (9)$$

Finally, the relation to σ_\pm is:

$$\sigma_\pm = \frac{\sigma}{2} \left(1 \pm \frac{4}{3} A_{\text{FB}} \right). \quad (10)$$

Taking Eq. (7) into account, Eqs. (8) and (9) show that the “conventional” observables simultaneously depend on all four contact interaction couplings and consequently do not allow a model-independent analysis, but only the simplified one-parameter fit of individual models mentioned above. Instead, as shown by Eqs. (4) and (5), the situation is definitely improved by considering the combinations σ_+ and σ_- , each one depending on just pairs of contact interaction parameters by construction. Consequently, such pairs of coupling constants can be separately constrained and furthermore, the combination of data on, respectively, σ_+ and σ_- at different energies will allow to further restrict such separate bounds in a model-independent way.

To this purpose, one has to quantitatively assess the sensitivity to the contact interaction couplings of σ_+ and σ_- , that ultimately will specify the “significance”, i.e., the attainable reach on these parameters for given experimental uncertainty on the basic observables. With $\mathcal{O} = \sigma_\pm$, such sensitivity can be defined as

$$\mathcal{S} = \frac{|\Delta\mathcal{O}|}{\delta\mathcal{O}}, \quad (11)$$

where $\Delta\mathcal{O} = \mathcal{O}^{SM+CI} - \mathcal{O}^{SM}$ represents the deviation from the SM prediction induced by the Lagrangian of Eq. (1) and $\delta\mathcal{O}$ is the corresponding experimental uncertainty, combining statistical and systematical uncertainties. In our application, we express σ_\pm^{SM} in terms of improved Born amplitudes [8, 9], such that the form of the previous formulae remains the same, with the values $m_{\text{top}} = 175$ GeV and $m_H = 100$ GeV. Regarding the experimental input, the values of σ_+ and σ_- as well as their uncertainties $\delta\sigma_+$ and $\delta\sigma_-$ are reconstructed

from the measured σ and A_{FB} at the different energies *via* Eq. (10). It can be seen that, to a very good approximation, the correlation between the uncertainties on σ and A_{FB} is negligible. In all numerical analyses, we take initial- and final-state radiation into account by the programs ZFITTER and ZEFIT [10] properly adapted to the present case of contact interactions, with the experimentally used cuts on the initially radiated photon energy.

Table 1: Integrated luminosity per experiment collected during the runs at TRISTAN, LEP1 and LEP2.

collider	E_{CM} (GeV)	\mathcal{L}_{int} [pb^{-1}]
Tristan [11]	58	300
LEP1 [12] Z line shape	peak-3	1
	peak-2	21
	peak-1	1
	peak+1	1
	peak+2	21
	peak+3	1
LEP2 [13]	130	3
	136	3
	161	10
	172	10
	183	53
	189	158
	192	25
	196	76
	200	83
	202	40

In Table 1, we show the energy points considered in the subsequent numerical analysis and the corresponding collected luminosities that determine the statistical uncertainties (in many cases dominant), referring for definiteness to the experiments DELPHI at LEP and VENUS and AMY at TRISTAN. As anticipated, our derivation of model-independent bounds on the contact interaction couplings will make use of the combinations of constraints at different energies. In Figs. 1-3, we show as a representative case the values of \mathcal{S} defined in Eq. (11) for given reference values $\epsilon_{\alpha\beta} = 5 \cdot 10^{-2}$, at the energy points listed in Table 1, and using the corresponding experimental uncertainties $\delta\sigma_{\pm}$.

Clearly, higher numerical values of \mathcal{S} indicate higher sensitivity to the relevant contact interaction parameter. One can easily see from the previous equations that the small values of \mathcal{S} around 90 GeV reflect the zero in the real part of the Z propagator at the peak, and that, in general, \mathcal{S} is small in the vicinity of a zero of SM amplitudes. Although being just illustrative examples, Figs. 1-3 indicate that the sensitivity significantly depends both on the reaction channel and, quite important, on the energy. Also, they show the role of data at “low” energy, where the sensitivity can be relatively high.

Indeed, assuming, as it is natural, that no deviations from the SM are observed within

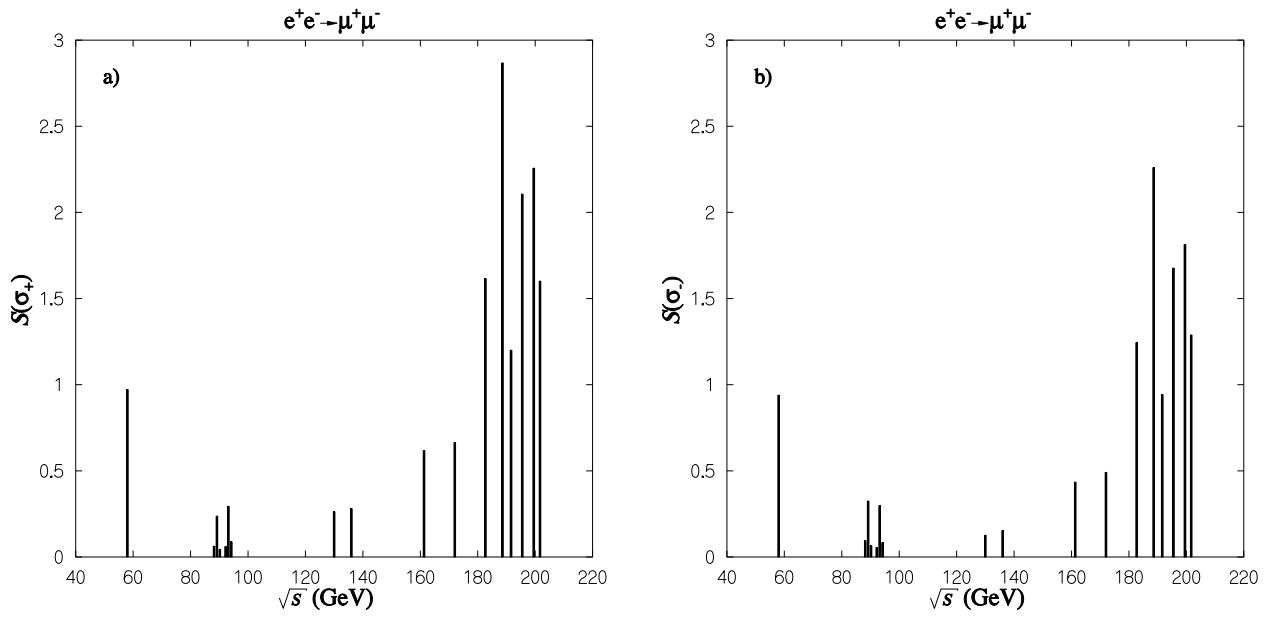


Figure 1: Sensitivity of the observables σ_{\pm} to contact interaction parameters $\epsilon_{RR} = 5 \cdot 10^{-2}$, $\epsilon_{LL} = 0$ (a) and $\epsilon_{RL} = 5 \cdot 10^{-2}$, $\epsilon_{LR} = 0$ (b) for the process $e^+e^- \rightarrow \mu^+\mu^-$ at the energy points listed in Table 1, and using the experimental uncertainties in Refs. [11, 12, 13]

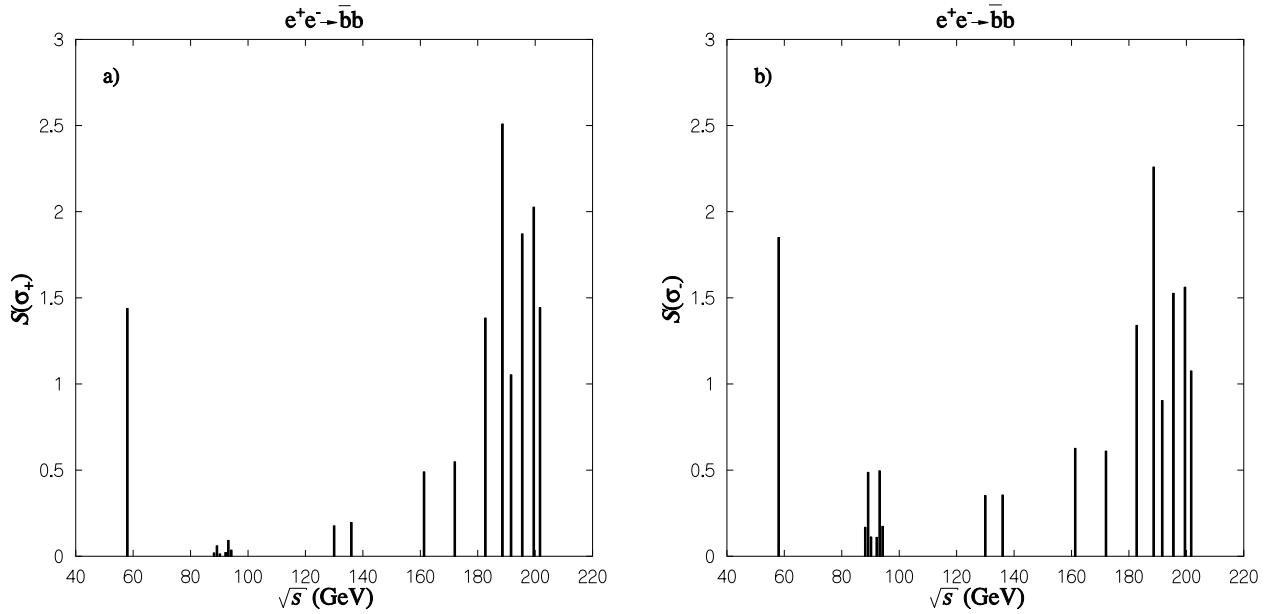


Figure 2: Same as Fig. 1, but for $e^+e^- \rightarrow b\bar{b}$.

the experimental accuracies, constraints on the contact interaction parameters $\epsilon_{\alpha\beta}$ can be obtained from the inequality

$$|\Delta\mathcal{O}| < \delta\mathcal{O}, \quad (12)$$

that, using Eqs. (4)-(7), in the planes $(\epsilon_{RR}, \epsilon_{LL})$ and $(\epsilon_{RL}, \epsilon_{LR})$ translates into the allowed

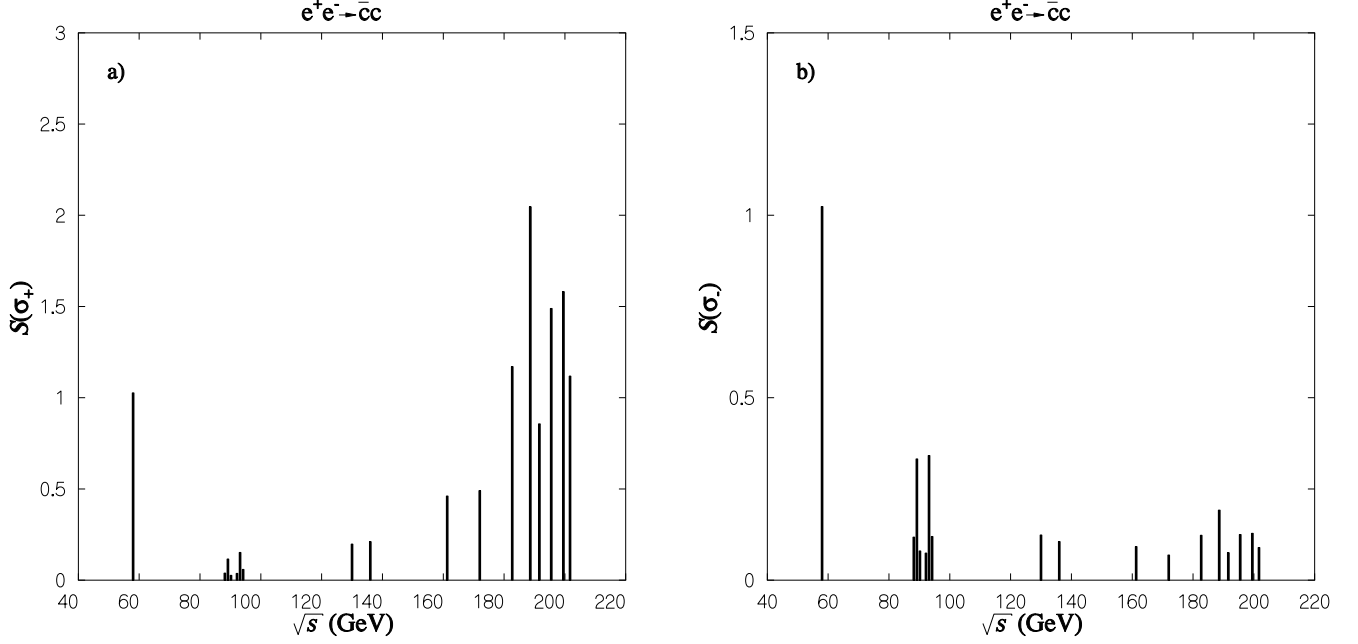


Figure 3: Same as Fig. 1, but for $e^+e^- \rightarrow \bar{c}c$.

areas enclosed by the concentric circles:

$$(\epsilon_{\alpha\beta} + a_{\alpha\beta})^2 + (\epsilon_{\alpha'\beta'} + b_{\alpha'\beta'})^2 = (a_{\alpha\beta})^2 + (b_{\alpha'\beta'})^2 \pm \kappa^2, \quad (13)$$

where $(\alpha\beta, \alpha'\beta') = (\text{LL}, \text{RR})$ and (LR, RL) for the cases of σ_+ and σ_- , respectively, and correspondingly:

$$a_{\alpha\beta} = \frac{\alpha_{e.m.}}{s} A_{\alpha\beta}^{SM}; \quad b_{\alpha'\beta'} = \frac{\alpha_{e.m.}}{s} A_{\alpha'\beta'}^{SM}; \quad \kappa^2 = \left(\frac{\alpha_{e.m.}}{s} \right)^2 \frac{4}{N_C \sigma_{pt}} \delta\sigma_{\pm}. \quad (14)$$

These relations show that both the centre and the radii of the circles $R_1, R_2 = \sqrt{a^2 + b^2 \pm \kappa^2}$ are determined by the SM helicity amplitudes and depend on energy, while the width of the allowed area is determined by the experimental uncertainty $\delta\sigma_{\pm}$.¹ Therefore, in principle, the combination of two (or more) such allowed regions at different energies can lead to a reduced allowed region and, ultimately, to model-independent bounds on the contact interaction coupling constants.

In practice, to perform such combination and derive the numerical constraints on $\epsilon_{\alpha\beta}$, we define a χ^2 as

$$\chi^2 = \sum_i \left(\frac{\Delta\mathcal{O}_i}{\delta\mathcal{O}_i} \right)^2, \quad (15)$$

where i runs over the 17 data samples collected at the different energies from 58 GeV to 202 GeV listed in Table 1, and, under the previous assumption that no deviations are shown by those data, we impose $\chi^2 < \chi_{\text{CL}}^2$, where the actual value of χ_{CL}^2 specifies the desired

¹Occasionally, depending on particular values of s and $\delta\sigma_{\pm}$, one might have $R_2 = 0$, in which case the allowed region is a circle of radius R_1 .

“confidence” level. As the two separate cases, σ_+ and σ_- , depend on two independent free parameters, we choose $\chi_{\text{CL}}^2 = 6$ as consistent with a two-parameter analysis. The resulting bounds are depicted in Figs. 4-6. In these figures, the dashed contours result from LEP2 data, dash-dotted ones correspond to TRISTAN data, the full line is obtained from combination of LEP1 and LEP2 results and, finally, the shaded area is the result of the combination of all experiments. One can clearly see the significant role of such combination of measurements at different energies in deriving a restricted, model-independent, region allowed to the contact interaction couplings around the SM point $\epsilon_{\alpha\beta} = 0$.

Indeed, the horizontal and vertical arms of the crosses in Figs. 4-6, intersecting at $\epsilon_{\alpha\beta} = 0$, may be considered as qualitative indications of bounds obtained by taking one non-zero contact interaction coupling at a time², a procedure testing the individual models. In this regard, we notice that, although on their own giving much less stringent bounds than LEP2 data in this kind of one-parameter analysis, the “low” energy TRISTAN data, when combined with the former ones, play an essential role in severely reducing the allowed area in the present model-independent procedure taking all contact coupling constants simultaneously into account.

Clearly, the analysis presented here is rather phenomenological, in the sense that numerical results are not derived by a conventional fitting procedure to σ_+ and σ_- . Nevertheless, since the available experimental data for σ and A_{FB} do not show deviations from the SM within the accuracies, we expect that the bounds on contact interaction parameters from such a fitting procedure would not significantly differ from those in Figs. 4-6.

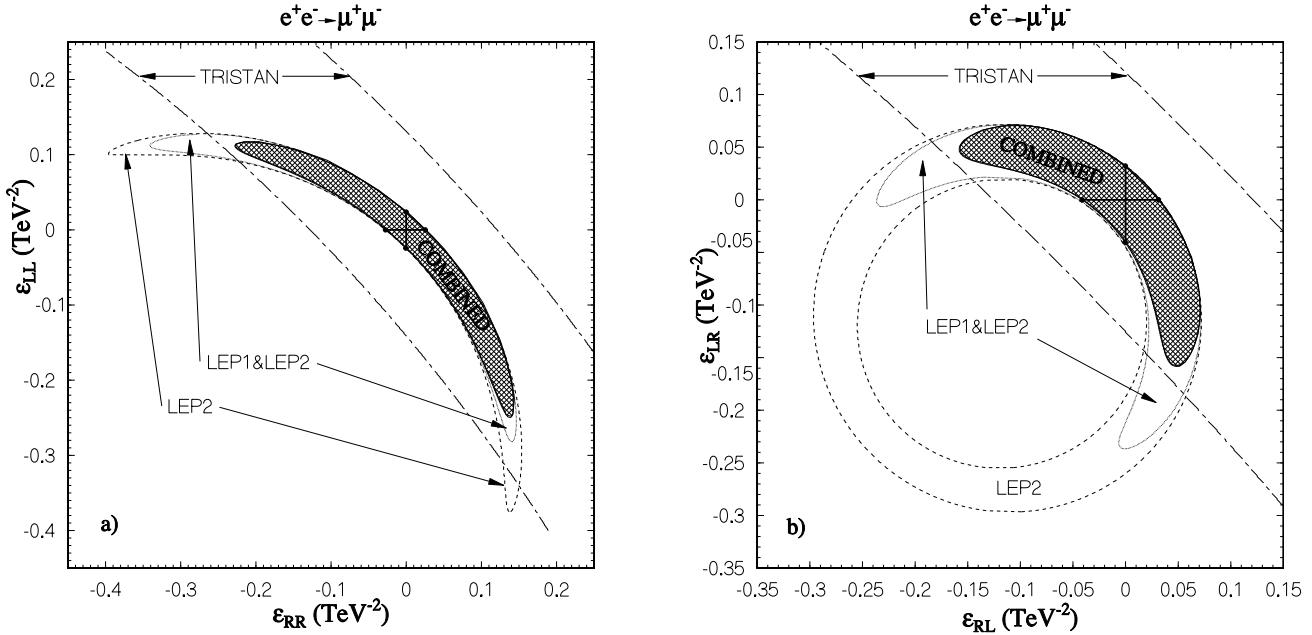


Figure 4: Allowed areas at 95% C.L. on leptonic contact interaction parameters in the planes $(\epsilon_{\text{RR}}, \epsilon_{\text{LL}})$ (a) and $(\epsilon_{\text{RL}}, \epsilon_{\text{LR}})$ (b), obtained from σ_+ and σ_- , respectively.

²Actually, in this one-parameter case, one should rescale the value of χ_{CL}^2 to $\chi_{\text{CL}}^2 = 4$.

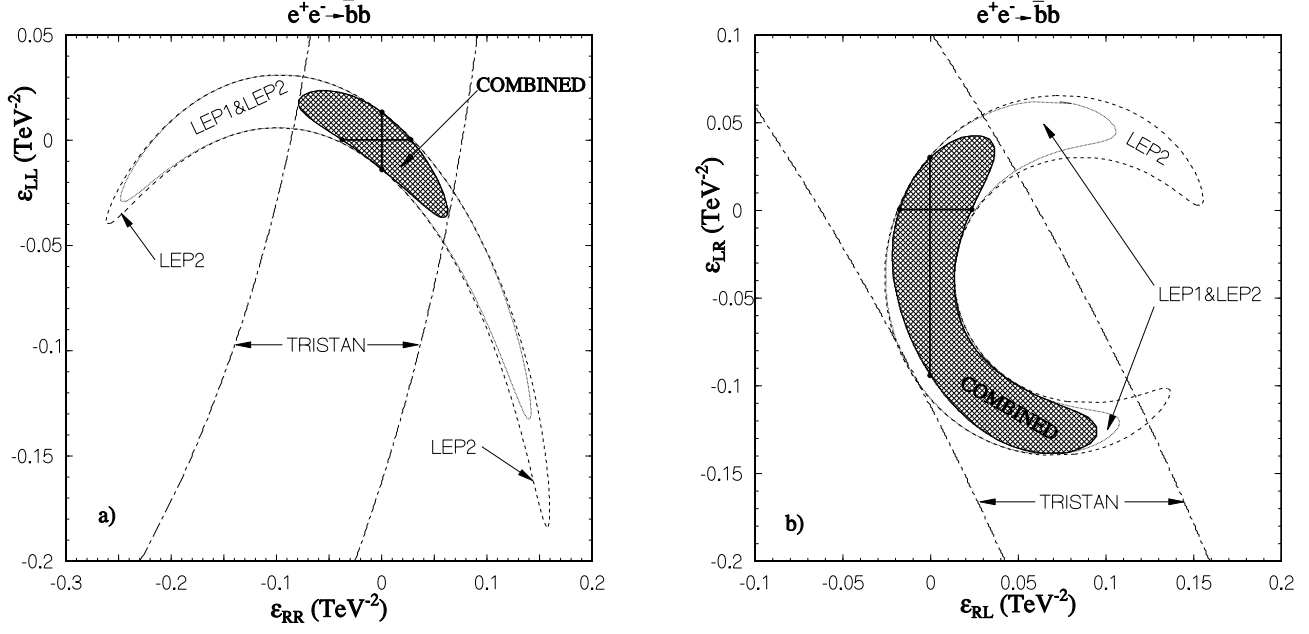


Figure 5: Same as Fig. 4, but for $e^+e^- \rightarrow b\bar{b}$.

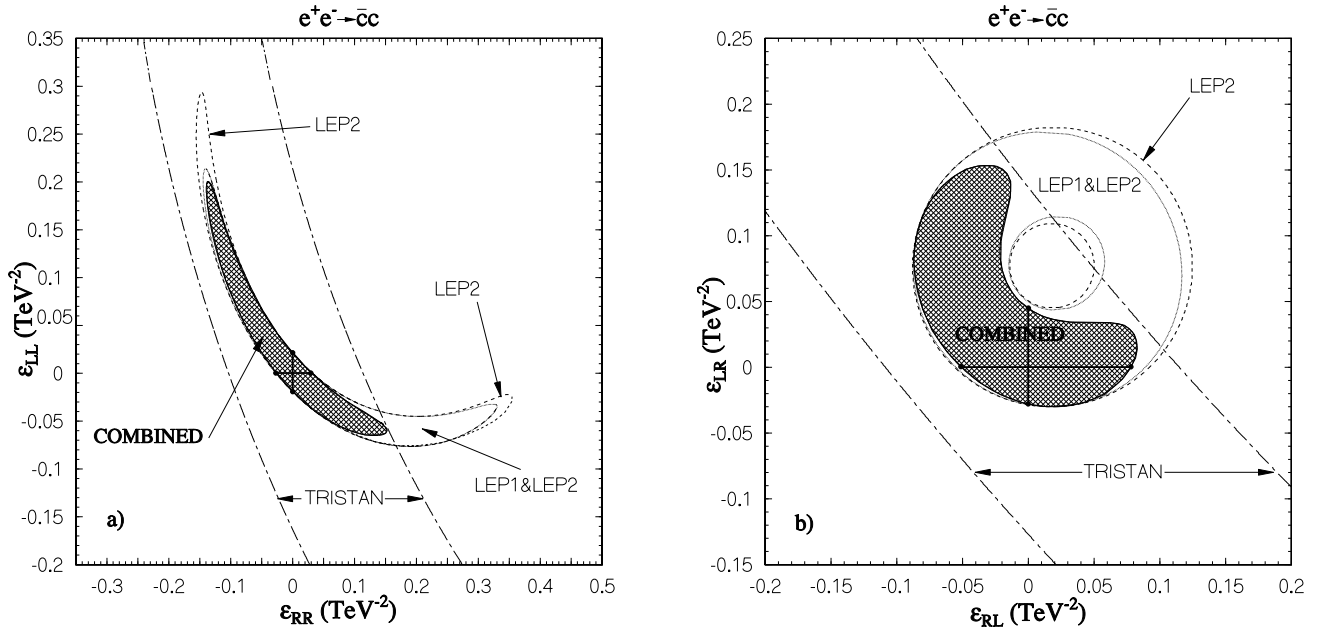


Figure 6: Same as Fig. 4, but for $e^+e^- \rightarrow c\bar{c}$.

References

- [1] See, e.g.: D. Abbaneo et al., The LEP Collaborations, CERN-EP-2000-016.
- [2] E. J. Eichten, K. D. Lane, M. E. Peskin, Phys. Rev. Lett. **50** (1983) 811;
R. Rückl, Phys. Lett. **B 129** (1983) 363.
- [3] V. Barger, K. Cheung, K. Hagiwara, D. Zeppenfeld, Phys. Rev. D **57** (1998) 391;
D. Zeppenfeld, K. Cheung, preprint MADPH-98-1081, hep-ph/9810277.
- [4] G. Altarelli, J. Ellis, G. F. Giudice, S. Lola, M. L. Mangano, Nucl. Phys. **B 506** (1997) 3;
R. Casalbuoni, S. De Curtis, D. Dominici, R. Gatto, Phys. Lett. **B 460** (1999) 135;
V. Barger, K. Cheung, Phys. Lett. **B 480** (2000) 149.
- [5] H. Kroha, Phys. Rev. D **46** (1992) 58.
- [6] A.A. Babich, P. Osland, A.A. Pankov, N. Paver, Phys. Lett. **B 476** (2000) 95; **B 481** (2000) 263.
- [7] B. Schrempp, F. Schrempp, N. Wermes, D. Zeppenfeld, Nucl. Phys. **B 296** (1988) 1.
- [8] M. Consoli, W. Hollik, F. Jegerlehner, *in* Z physics at LEP1, G. Altarelli, R. Kleiss, C. Verzegnassi (Eds.), vol.1, p.7, 1989.
- [9] G. Altarelli, R. Casalbuoni, D. Dominici, F. Feruglio, R. Gatto, Nucl. Phys. **B 342** (1990) 15.
- [10] S. Riemann, FORTRAN program ZEFIT Version 4.2;
D. Bardin et al., preprint DESY 99-070, hep-ph/9908433.
- [11] M. Miura et al., Phys. Rev. D **57** (1998) 5345;
T. Arima et al., Phys. Rev. D **55** (1997) 19;
K. Ueno et al., Phys. Lett. **B 381** (1996) 365;
D. Stuart et al., Phys. Rev. D **49** (1994) 3098;
K. Abe et al., Phys. Lett. **B 313** (1993) 288.
- [12] P. Abreu et al., Eur. Phys. J. **C10** (1999) 219;
P. Abreu et al., preprint DELPHI 98-113 CONF 175;
D. Abbaneo et al., The LEP/SLD Heavy Flavour Working Group, preprint DELPHI 98-54 CONF 246.
- [13] P. Abreu et al., preprint CERN-EP/2000-068;
K. Cieřlik et al., preprint DELPHI 2000-038 CONF 356;
K. Cieřlik et al., preprint DELPHI 2000-129 CONF 428;
A. Behrmann et al., preprint DELPHI 2000-036 CONF 355;
P. Abreu et al., Eur. Phys. J. **C11** (1999) 383;
A. Behrmann et al., preprint DELPHI 99-58 CONF 247.